



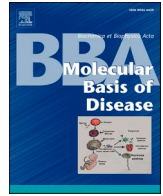
Since January 2020 Elsevier has created a COVID-19 resource centre with free information in English and Mandarin on the novel coronavirus COVID-19. The COVID-19 resource centre is hosted on Elsevier Connect, the company's public news and information website.

Elsevier hereby grants permission to make all its COVID-19-related research that is available on the COVID-19 resource centre - including this research content - immediately available in PubMed Central and other publicly funded repositories, such as the WHO COVID database with rights for unrestricted research re-use and analyses in any form or by any means with acknowledgement of the original source. These permissions are granted for free by Elsevier for as long as the COVID-19 resource centre remains active.



Contents lists available at ScienceDirect

BBA - Molecular Basis of Disease

journal homepage: www.elsevier.com/locate/bbadis

The *Drosophila melanogaster* ACE2 ortholog genes are differently expressed in obesity/diabetes and aging models: Implications for COVID-19 pathology

Tâmie Duarte^a, Mônica de Medeiros Silva^a, Paula Michelotti^a,
Nilda Berenice de Vargas Barbosa^a, Bruno César Feltes^{b,c}, Márcio Dorn^{b,d,e},
João Batista Teixeira da Rocha^a, Cristiane Lenz Dalla Corte^{a,*}

^a Department of Biochemistry and Molecular Biology, Natural and Exact Sciences Center, Federal University of Santa Maria, 1000 Roraima Avenue, Santa Maria, RS 97105-900, Brazil

^b Institute of Informatics, Federal University of Rio Grande do Sul, 9500 Bento Gonçalves Avenue, Porto Alegre, RS 91501-970, Brazil

^c Institute of Biosciences, Federal University of Rio Grande do Sul, 9500 Bento Gonçalves Avenue, Porto Alegre, RS 91501-970, Brazil

^d Center of Biotechnology, Federal University of Rio Grande do Sul, 9500 Bento Gonçalves Avenue, Porto Alegre, RS 91501-970, Brazil

^e National Institute of Science and Technology - Forensic Science, 6681 Ipiranga Avenue, Porto Alegre, RS 90619-900, Brazil

ARTICLE INFO

Keywords:

Risk factors
COVID-19
ACE2
Ance
Acer
Molecular docking

ABSTRACT

The Spike glycoprotein of SARS-CoV-2, the virus responsible for coronavirus disease 2019, binds to its ACE2 receptor for internalization in the host cells. Elderly individuals or those with subjacent disorders, such as obesity and diabetes, are more susceptible to COVID-19 severity. Additionally, several SARS-CoV-2 variants appear to enhance the Spike-ACE2 interaction, which increases transmissibility and death. Considering that the fruit fly is a robust animal model in metabolic research and has two ACE2 orthologs, Ance and Acer, in this work, we studied the effects of two hypercaloric diets (HFD and HSD) and aging on ACE2 orthologs mRNA expression levels in *Drosophila melanogaster*. To complement our work, we analyzed the predicted binding affinity between the Spike protein with Ance and Acer. We show for the first time that *Ance* and *Acer* genes are differentially regulated and dependent on diet and age in adult flies. At the molecular level, Ance and Acer proteins exhibit the potential to bind to the Spike protein in different regions, as shown by a molecular docking approach. Acer, in particular, interacts with the Spike protein in the same region as in humans. Overall, we suggest that the *D. melanogaster* is a promising animal model for translational studies on COVID-19 associated risk factors and ACE2.

1. Introduction

Obesity, diabetes mellitus (DM), and elderly individuals are associated with increased susceptibility to infection and progression of Severe Acute Respiratory Syndrome Coronavirus 2 (SARS-CoV-2), responsible for the coronavirus disease 2019 (COVID-19). After the first detection in Wuhan, China, it quickly spread worldwide and was declared a pandemic by the World Health Organization (WHO) [1–5]. The entry of SARS-CoV-2 into the host cell is through its binding to the angiotensin-converting enzyme 2 (ACE2), similar to the previous coronavirus SARS-CoV [5–9]. ACE2 and its angiotensin-converting enzyme (ACE) homologue perform as a significant component of the renin-angiotensin-aldosterone system (RAAS), a dynamic system in vascular function, blood pressure, and immune response regulation. The enzymatic activity of ACE2 is associated with the degradation of Angiotensin II (Ang II) to

Angiotensin 1-7 (Ang 1-7), stimulating vasodilation and anti-inflammatory effects and, to a lesser extent, cleaving Angiotensin I (Ang I) to Angiotensin 1-9 (Ang 1-9). Adversely, ACE converts Ang I to Ang II, a potent vasoconstrictor and pro-inflammatory agent [5–7].

Initially, higher ACE2 protein levels were considered the main cause of the susceptibility to SARS-CoV-2 infection [5,8,10]. However, conflicting data show that patients with COVID-19 complications also had an increased pro-inflammatory profile and reduced ACE2 baseline levels associated with upregulation of Ang II and downregulation of Ang-(1-7) levels [7,8]. Among the available hypothesis, it is thought that people in the risk group have an imbalance between ACE and ACE2 activity that leads to pro-inflammatory responses, predisposing them to cytokine storm syndrome [8]. Furthermore, the quickly SARS-CoV-2 propagation has triggered mutations in its genetic code at a fast rate: studies based on genome sequencing have identified at least 13 coronavirus variants

* Corresponding author at: Federal University of Santa Maria, 1000 Roraima Avenue, Santa Maria, RS 97105-900, Brazil.

E-mail address: cristiane.corte@ufsm.br (C.L. Dalla Corte).

<https://doi.org/10.1016/j.bbadis.2022.166551>

Received 6 May 2022; Received in revised form 8 August 2022; Accepted 12 September 2022

Available online 15 September 2022

0925-4439/© 2022 Elsevier B.V. All rights reserved.

[11,12]. To date, it is known that most mutations occur in the Spike protein, and some of the variants are more transmissible and lethal than others [11,13]. The lack of knowledge about COVID-19 variants and the relationship of the RAAS system underscores the need for continued RAAS system research, especially on the most vulnerable groups of individuals.

The fruit fly *Drosophila melanogaster* is a model organism with wide availability of genetic tools, high similarity of virus pathways compared to vertebrates, and the possibility of therapeutic drug discovery [6,14,15]. Remarkably, *D. melanogaster* expresses two catalytic orthologs of ACE and ACE2, the angiotensin-converting enzyme (Ance) and angiotensin-converting enzyme related (Acer) [6,16]. For this reason, the fruit fly has been discussed in several reviews as a potential animal model for COVID-19 research [6,14,17], although, it has been overlooked in experimental COVID-19 research so far. Therefore, in the present study, we investigated the *Ance* and *Acer* mRNA expression levels in fruit fly models of obesity/DM and aging, that reproduce risk factors for COVID-19. Additionally, we analyzed the *Ance* and *Acer* proteins' binding affinity with the SARS-CoV-2 Spike protein by molecular docking. In this way, this investigation helps to elucidate the relationship between the COVID-19 risk groups and the RAAS system and the possibility of using this organism for *in vivo* and *ex vivo* studies related to COVID-19 and other coronaviruses.

2. Methods and materials

2.1. Flies and housing

In this study, we used the Oregon-R wild-type strain of *D. melanogaster* (female and male), maintained in an incubator at a constant temperature (25 °C) with 40–55 % humidity and a 12:12 h light-dark photoperiod. Adult flies were collected at 0–3 days of age (post-eclosion) and transferred to a separate vial containing the different experimental diets for three or forty days, depending on the group. At the end of each protocol, flies were anesthetized on ice and weighed ($n = 5$).

2.1.1. Obesity and diabetes model

To induce obesity and DM in flies, we used two food diets: the high-fat diet (HFD) and the high-sugar diet (HSD), as illustrated in Table 1. Based on previous studies, the diets contain 30 % of margarine and 30 % of sucrose, respectively [18–20]. The experimental tests were performed after three days. To validate our models, we performed the analysis of body weight, glucose and triglyceride amount, as well as *InR* and *dilp5* mRNA expression levels, two markers of insulin resistance.

2.1.2. Aging model

The aging flies used in this work had 40 days old (post-eclosion) and were transferred into a new food (CD) every two days, separated by sex [21].

2.2. Triglyceride, glucose, and protein measurements

After three days of exposure to the diets, we separated five whole

Table 1

Content and energetic value of control (CD), aging, high-fat (HFD), and high-sugar (HSD) diet.

Ingredients	CD and Aging	HFD	HSD
Agar (g)	1.5	1.5	1.5
Sucrose (g)	5	5	30
Yeast (g)	10	10	10
Margarine (g)	0	30	0
Nipagin 10 % (mL)	3	3	3
Propionic acid (mL)	0.3	0.3	0.3
Total kcal	58.3	274.3	158.3

flies and prepared them as described by Tennessen et al. [22]. We used the Serum Triglyceride Determination Kit (Sigma-Aldrich, Saint Louis, MO) and the Glucose GO Assay Kit (Sigma-Aldrich, Saint Louis, MO) to measure triglycerides (TAG) and glucose levels according to the manufacturer's instructions. Approximately 20–30 flies were used for hemolymph TAG and glucose levels analysis, as described by Ecker et al. [20], with a few modifications: Flies were left without food for at least 2 h before TAG and glucose level analysis. For hemolymph extraction, the samples were frozen 2× in nitrogen liquid and centrifuged at 13,000 rpm for 10 min at 4 °C. We measured spectrophotometrically at 540 nm. Although Hildebrandt et al. [23] demonstrate that absorbance at 540 nm does not detect eye pigment color, we performed a blank (no color reagent) for each sample. All tests were normalized with the respective homogenate protein concentrations as determined by the Bradford [24] method, using bovine serum albumin as the standard.

2.3. Climbing assay

The locomotion of *D. melanogaster* was determined using the climbing test described previously by Jimenez-Del-Rio et al. [25] with some modifications. Groups of 10 flies were anesthetized on the ice during 1–2 min to immobilization and transferred to glass tubes (length, 20 cm; diameter, 2 cm). After 30 min at room temperature (25 °C) for recovery, the flies were gently tapped to the bottom of the tube and allowed to climb up for 10 s. Climbing ability was determined as the average height reached by flies in each tube, and results were expressed as the mean of trials repeated three times at 1-minute intervals.

2.4. RNA isolation and RT-PCR

Whole bodies of 20 flies per group (CD, HFD, HSD, and aging separated by sex) were used to measure *InR*, *dilp5*, *Ance*, *Acer*, and β -*Actin* mRNA expression levels by the real-time reverse transcription-polymerase chain reaction (RT-PCR). Total RNA was extracted using TRIzol (Invitrogen, Brazil), according to the manufacturer's instructions. The quantification was performed using NanoDrop™ 2000/2000c Spectrophotometer (Thermo Fisher Scientific) and analyzed with the Desjardins and Conklin [26] protocol. For RNA purification, we treated the samples with DNase I (Invitrogen, Brazil), and synthesized cDNA with the Applied Biosystems™ High-Capacity cDNA Reverse Transcription Kit (Thermo Fisher Scientific). Subsequently, we used a thermocycler (Applied Biosystems) to incubate the samples according to the manufacturer's instructions. RT-PCR was performed with 5 μ L of PowerUp SYBR Green MasterMix (Thermo Fisher Scientific), 4.4 μ L of a sample containing 100 ng/ μ L of cDNA, 0.3 μ L of forward and reverse primer [30 μ M], and 0.3 μ L of DEPC-treated water. StepOnePlus Real-Time PCR System (Applied Biosystems) was used to load the samples, with the following cycling protocol: 2 min at 50 °C, 2 min at 95 °C finished by 40 cycles of 15 s at 95 °C, and 1 min at 60 °C. Melting curve analysis (15 s at 95 °C and 1 min at 60 °C) was used to determine specific amplification products and the possible formation of primer dimers. We analyzed all samples as triplicates with negative control and manually determined the CT (cycle threshold) value using StepOne Software v2.3 (Applied Biosystems, NY). We utilized the 2^{-DDCT} [27] method to calculate mRNA normalization with the β -*Actin* mRNA expression levels.

2.5. Primers design

Forward and reverse primers were designed using National Center for Biotechnology Information (NCBI) (<https://www.ncbi.nlm.nih.gov/>), BLAT - UCSC Genome Browser (<https://genome.ucsc.edu/cgi-bin/hgBlat>) and OligoAnalyzer™ Tool (<https://www.idtdna.com/pages/tools/oligoanalyzer>). The primers' sequences are shown in Table 2.

Table 2
Primer sequences.

Gene		Primer Sequence
<i>InR</i>	Forward	GTTTCGTCGTGCGGAAAATCA
	Reverse	CATTCACGAAATGCTGGGGC
<i>dilp5</i>	Forward	GCGGATTTGGATAGCTCCGA
	Reverse	AAAGGAACACGATTTCGCGG
<i>Ance</i>	Forward	CGGTCACGTTTCGATTGGTTG
	Reverse	GGTTACCGCCAAAGTAGCCA
<i>Acer</i>	Forward	ACTCGCGCAGCAGATAAAGCT
	Reverse	CCCAATTGGATAGGTGCTCG
β -Actin	Forward	TCGATCATGAAGTGGCAGCT
	Reverse	ACCGATCCAGACGGAGTACT

2.6. Molecular docking

We use protein docking to predict protein-protein binding affinities between *Ance* and *Acer* proteins and Spike protein. The binding models were generated by ClusPro 2.0 protein-protein docking server [28,29] and studied using PyMol software (<https://pymol.org>). ClusPro follows three computational steps: (i) rigid-body docking using the fast Fourier transform (FFT) correlation approach, (ii) root mean square deviation (RMSD)-based clustering to find the largest cluster that will represent the likely models of the complex and (iii) refinement of selected structures. We chose the Spike protein PDB ID 6VSB [30] and the *Ance* PDB ID IJ36 [31] to perform the docking analysis. Nevertheless, *Acer* crystallographic structure is not available in the Protein Data Bank. Hence, we use the *Acer* 3D structure predicted by Alpha Fold (<https://alphafold.ebi.ac.uk/entry/Q9VLJ6>) [32]. We remove unstructured terminal residues from all proteins and predict complexes considering four scoring schemes: (i) balanced, (ii) electrostatic-favored, (iii) hydrophobic-favored, and (iv) *van der Waals* + electrostatics. The protein complex of the largest cluster from the balanced scoring schema was used for further analysis.

2.7. Data analysis

Statistical analysis was done using an unpaired *t*-test. Concerning comparison between treatments, a one-way analysis of variance (ANOVA) followed by a Tukey comparisons test was used. For comparisons between treatment and sex, a two-way ANOVA was performed, followed by Sidak's multiple comparisons test. The correlation was analyzed by Pearson's correlation coefficients. The normality of data and homogeneity of variances were analyzed using the Shapiro-Wilk test, and results were expressed as means \pm standard error of means (S.E.M.). The data were analyzed using GraphPad Prism 8.0 (GraphPad Software, San Diego California USA, www.graphpad.com), and all significances were set at $p \leq 0.05$.

3. Results and discussion

Epidemiological studies of COVID-19 revealed that individuals with obesity, DM, and advanced age have a higher susceptibility to severe infections and mortality [1,3,4]. In addition, obesity and DM are major public health concerns affecting >650 million people worldwide and are known to alter the RAAS system, often treated with ACE inhibitors (ACEI) [8,10,33]. In this context, the present work aimed to investigate risk factors for COVID-19 and ACE/ACE2 through a translational study using the fruit fly as an organism model. It is well-reported that the main metabolic pathways that regulate energy homeostasis are highly conserved in the fruit fly. For example, a high lipid or sugar content in fruit fly food could induce hyperlipidemia, hyperglycemia, body weight gain, and insulin resistance, like in humans [18,34–36]. Concerning the food composition of fruit flies, such as types and concentrations of ingredients, there is a high variability in previous animal studies [18,20,21,34]. Therefore, the first step was to standardize two diets to

induce obesity and DM in adult *D. melanogaster* based on previous studies with high content of lipids and sugar [18,20,21]. Since we intended to investigate the *Ance* and *Acer* mRNA expression levels in three groups (high fat, high sugar, and aging), we used the same dietary basis for all models.

It is noteworthy that typical obesity models use coconut oil as a fat source [34,36]. However, many flies did not survive when we used this substance due to coconut oil making the medium less homogeneous and more humid (data not shown). Nevertheless, considering a prior study by Musselman et al. [18] that utilized hydrogenated shortening as a fat source, we tested margarine, a similar ingredient. Concerning sugar, we chose sucrose since it is the most common sugar and is used in our control diet (CD), based on *D. melanogaster* aging studies [19]. Also, we used an equal feed period for HFD and HSD, aiming to prevent a possible interfering factor in the results. To analyze diets efficacy, we: (i) weighed the fruit flies; (ii) analyzed glucose and triglyceride amount in the total body also hemolymph; and then (iii) evaluated the insulin receptor (*InR*) and *Drosophila* insulin-like peptide 5 (*dilp5*) mRNA expression levels, two essential genes involved in the metabolic insulin signaling pathway.

3.1. Diets models produce obesity and diabetes phenotypes

In humans, obesity is defined as an excessive body fat accumulation, and the most common parameter employed for its diagnosis is the Body Mass Index (BMI). Generally, obesity is associated with an elevated risk of developing metabolic abnormalities, including DM, characterized by high sugar blood concentrations [35]. At the onset, as obesity and DM parameters, we investigated the effects of HFD and HSD on weight, stored fat (triglycerides), and glucose levels. Both diets produced weight gain in females (Fig. 1A) and male flies (Fig. 1B). Other previous studies with HFD and HSD displayed an increased fly body mass [34,37].

Regarding the effects of HFD and HSD on glucose and triglyceride levels, no significant change in glucose total body levels was observed (Fig. 2A and B). However, there was an increase up to three times in glucose when assessed in the hemolymph, most significantly for flies on HSD (Fig. 2C and D). The factor that may have contributed to this result is on account of lipids are less efficiently converted into glucose compared to sucrose [38]. Moreover, we found an increase in the TAG levels in the total body (Fig. 2E and F) and hemolymph (Fig. 2G and H) of all groups. Earlier studies with high-fat and high-sugar diets also showed hyperlipidemia and hyperglycemia in adult fruit flies [18,20,34,36]. These results support the efficacy of HFD and HSD to induce obesity/DM in flies.

3.2. Aging flies reduced locomotion

The lifespan of wild-type flies at 25 °C is approximately 60 days [39]. Despite the short life span, the survival curves of *D. melanogaster* include the "youth" period (0–30 days) with a low mortality rate, the "old age" period (30–60 days) when the survival rate starts to drop rapidly, and "extreme old age" period (60–80 days) [39,40]. In vertebrates, aging is associated with several age-related functional deficits, such as locomotor impairments [25,40,41]. It is well established that flies exhibit age-dependent locomotor dysfunction, measured through the climbing ability. The climbing assay takes advantage of fruit flies negative geotaxis, a natural tendency to climb upwards against gravity [25,40]. Since locomotor behavior naturally decreases with age, we analyze the climbing behavior of the *D. melanogaster* at 3, 20, 30, and 40 days old, as a marker of aging. As expected, the climbing capacity steadily decreased in older flies: nearly 70 % at 30 days and 80 % at 40 days lower climbing activity than in the youngest flies (3 and 20 days) in both sexes (Fig. 3). This pattern agrees with the findings of earlier studies, which used the geotaxis behavior of flies to demonstrate the decreasing capacity of aging flies to climb vertical walls indicating locomotor deficits [40,41].

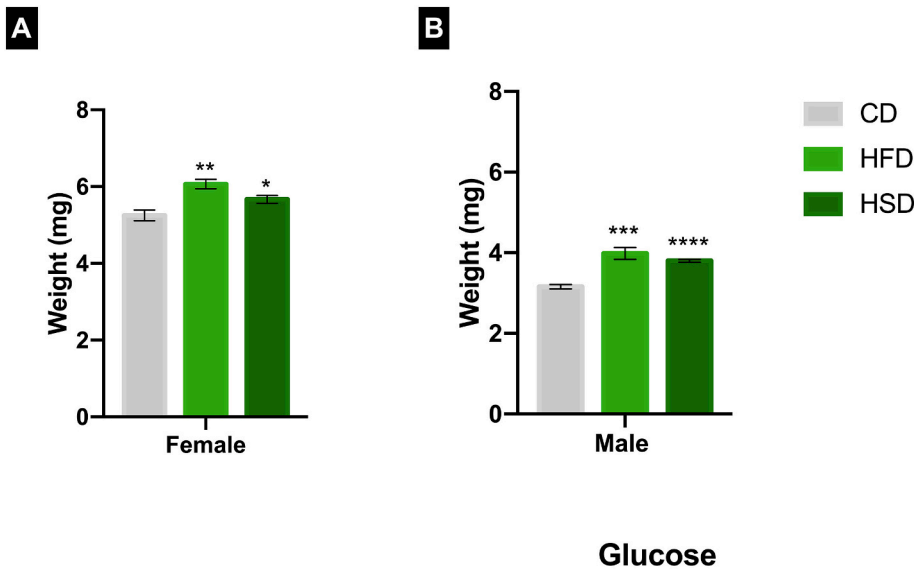


Fig. 1. HFD and HSD induces weight gain and aging decreases locomotion. (A) adult females and (B) adult males ($n = 15-20$ per experimental group). Errors bars indicated means \pm S.E.M. Significance between values for each experimental group and control was determinate with a *t*-test (Fig. 1A and B). Significance between relative abundance values was determined with a two-way analysis of variance (ANOVA) followed by Sidak's multiple comparisons test (Fig. 1C), * = $p < 0.05$, ** = $p < 0.01$, *** = $p < 0.001$ and **** = $p < 0.0001$.

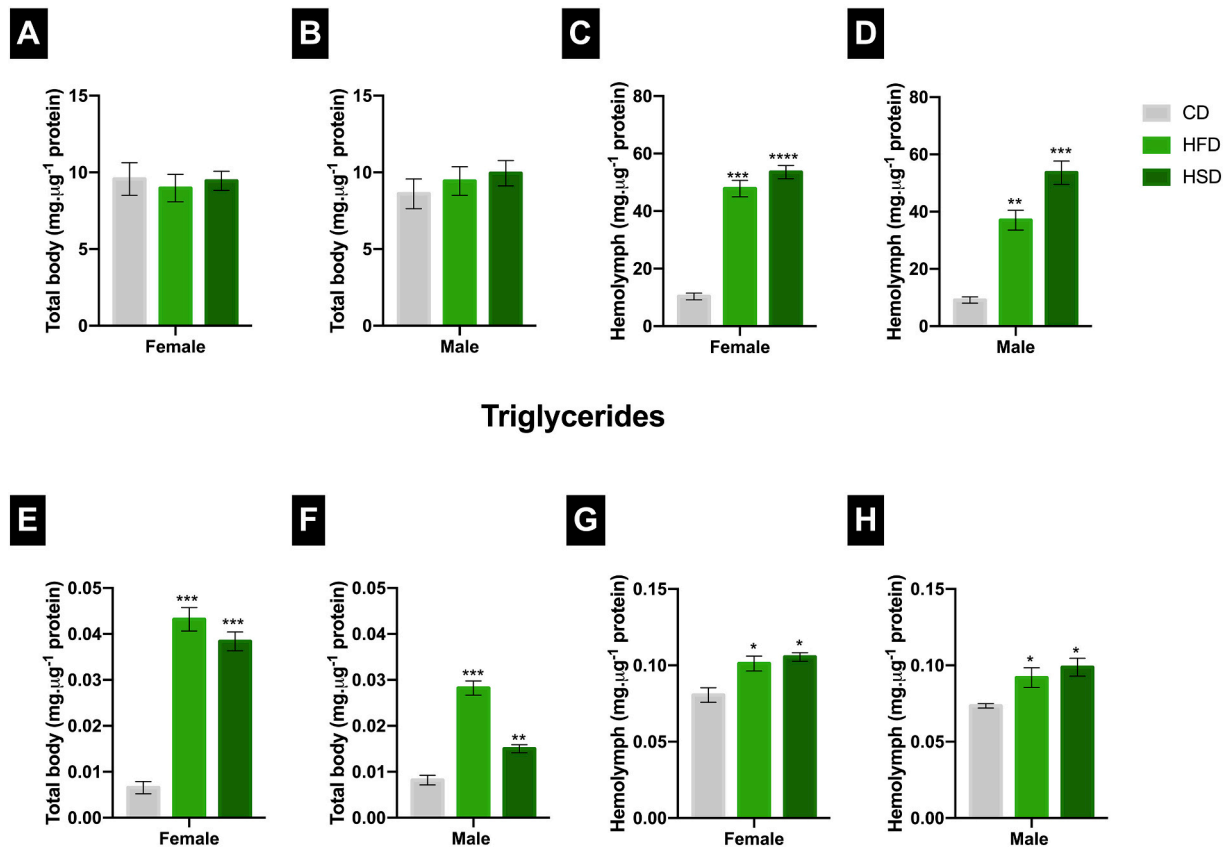


Fig. 2. Effects of HFD and HSD on triglycerides and glucose levels. Measures of TAG levels in total body on (A) females and (B) males, TAG levels in hemolymph of (C) females and (D) males, glucose levels in the total body of (E) females and (F) males, glucose levels in hemolymph of (G) females and (H) males ($n = 3$ per experimental group). Errors bars indicated means \pm S.E.M. Significance between values for each experimental group and control was determinate with a *t*-test, * = $p < 0.05$, ** = $p < 0.01$, *** = $p < 0.001$ and **** = $p < 0.0001$.

3.3. High fat and sugar diets disrupt the insulin pathway

The adipose fly body is a multifunctional organ involved in hormone secretion, with functional similarities to the vertebrate liver and adipose tissue [42]. Therefore, it also regulates nutrient-sensitive hormones, including insulin [18]. Insulin is an anabolic hormone stimulated by increased blood glucose, with action in skeletal muscle, liver, and

adipose tissue. Hyperglycemia and hypertriglyceridemia shown in our work (Fig. 2C, D, E, F, G, and H) could lead to failure to secrete or recognize this hormone [8]. The insulin receptor (IR) is responsible for recognizing insulin or insulin-like peptides (ILPs) [43]. Despite some differences, vertebrate and invertebrate IR are equivalent and activated by similar mechanisms. In the fruit flies, the insulin receptor is the insulin-like receptor (InR). While vertebrates have only one gene

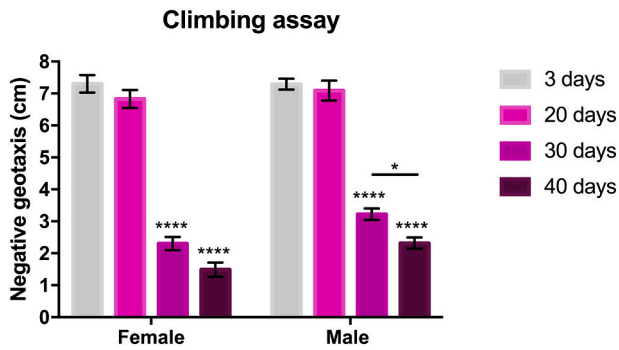


Fig. 3. Effect of aging on locomotor activity. Adult flies at 3, 20, 30, and 40 days old ($n = 10\text{--}15$ per experimental group). Errors bars indicated means \pm S.E.M. Significance between values for each experimental group and control was determined with a t -test. Significance between relative abundance values was determined with a two-way analysis of variance (ANOVA) followed by Sidak's multiple comparisons test, $* = p < 0.05$, and $**** = p < 0.0001$.

responsible for insulin production, the *D. melanogaster* genome encodes eight insulin-like peptides (Ilp1–8). Ilp1–7 interacts with only one InR, and among them, Ilp2–3 and 5 have particular importance for glycemic control due to acting similarly to human insulin [18,43,44].

To investigate HFD and HSD's role in nutrient-sensitive responses, we measured the *InR* and *dilp5* mRNA expression levels by RT-PCR. Both diets showed a decrease in the two genes, except for females fed with HSD, with a significant 2-fold difference in HFD compared to HSD for *InR* in males and *dilp5* in females (Fig. 4). Previous studies with HFD and HSD in adult flies demonstrated reduced insulin/insulin-like signaling (IIS), including *InR* and *dilp5* [37,42]. This IIS dysfunction induced by diets in flies resembles the corresponding pathway dysregulations in obese and diabetic humans, which occurs as a depletion in the insulin receptors, associated with insulin resistance [8,44]. Consistent with the literature, our data suggest that the HFD and HSD tested in this work are

suitable models for obesity and DM studies.

3.4. Risk groups from COVID-19 alter differently *Ance* and *Acer* genes expression

In humans, the *ACE* gene encodes two proteins with homologous domains: ACE and ACE2. On the other hand, *D. melanogaster* has six *Ace* genes encoding ACE orthologs, of which only *Ance* and *Acer* genes encode for proteins predicted to have zinc-metalloproteinase activity [16,45]. This feature makes *Acer* and *Ance* proteins similar to mammalian ACE and ACE2, thus classifying them as "ACE-like enzymes" [6]. ACE is a widely prescribed target of many antihypertensive drugs, while the ACE2 potential as a therapeutic target has only recently emerged given its involvement as a receptor for coronaviruses, including SARS-CoV-2 [6,9]. Through its function in the RAAS system, ACE2 plays a dual role in COVID-19 infections: as a receptor for the virus and an anti-inflammatory protective molecule. There is significant controversy about whether ACE2 overexpression would facilitate infection or restrict the disease process manifestations. Thus, positive or negative ACE2 regulation can have adverse consequences for the body. Changes in the ACE2 mRNA expression level and its regulatory mechanism before and after Spike protein binding to the ACE2 receptor remain unclear. Therefore, it is crucial to investigate the ACE and ACE2 mRNA expression levels and their relationship with coronavirus transmission and infection pathways to understand the pathogenesis and treatment options for COVID-19.

One limitation of the present study is that *D. melanogaster* has no conserved RAAS substrates, which could raise questions about the *Ance* and *Acer* functions *in vivo* in this organism. However, the phenotypes observed in *Ance* and *Acer* disruption are remarkably similar to those observed in models with conserved RAAS, such as the murine models [6,10,33]. Moreover, ACE and ACE2 share many features with *Ance* and *Acer*. In line with this, a work conducted by Lubbe et al. [9] demonstrated that *Ance* and *Acer* have ACE endopeptidase activity conserved, and Liao et al. [43] showed that ACE2 and *Acer* share the same cardiac

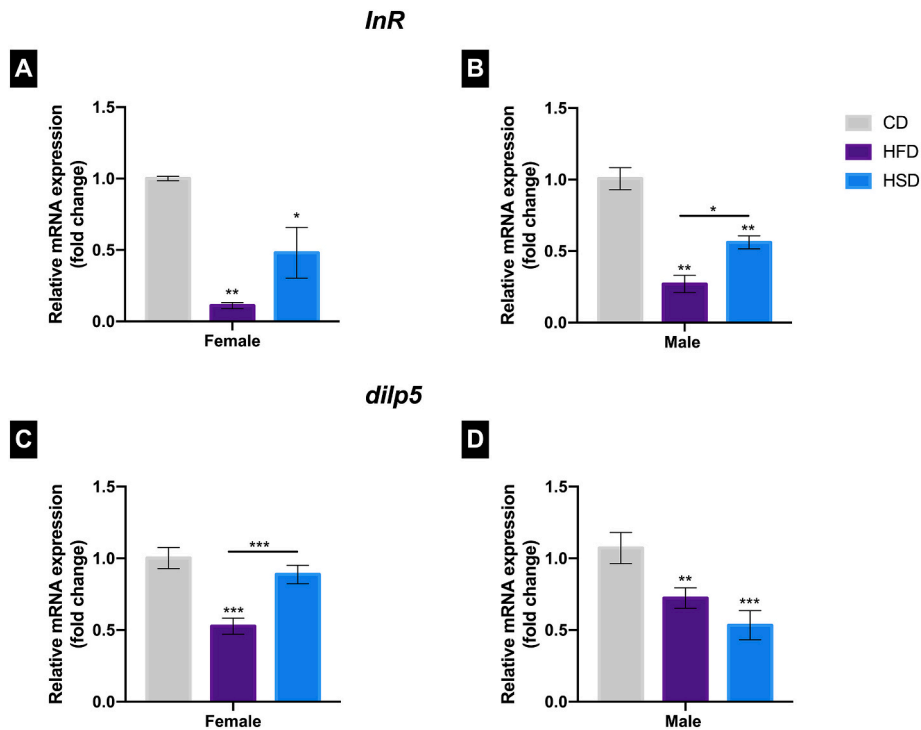


Fig. 4. Effects of HFD and HSD on *D. melanogaster* relative mRNA expression levels of (A) *InR* and (B) *dilp5* after three days of feeding. Errors bars indicated means \pm S.E.M., $n = 3\text{--}5$ per experimental group. Significance between relative abundance values was determined with a one-way analysis of variance (ANOVA) followed by a Tukey comparisons test, $* = p < 0.05$, $** = p < 0.01$, and $*** = p < 0.001$.

functions. Noteworthy, both *D. melanogaster* orthologs are effectively used in studies with ACE inhibitors [46,47]. Similar to ACE and ACE2, Ance and Acer also have a few distinct biophysical and biochemical properties. For example, while Ance can convert Ang I to Ang II with a catalytic efficiency, Acer does not cleave Ang I even at enzyme concentrations eight times higher than that required for 25 % hydrolysis by Ance. These two enzymes can hydrolyze the bradykinin, a vasodilator peptide, although Acer is less effective than Ance and ACE [6,16]. To date, only one study analyzed these two genes' mRNA expression levels, conducted during pupal development in fruit flies [16]. Likewise, ACE2 expression in human subcutaneous adipose tissue could be regulated by dietary changes [2,10]. For these reasons, we evaluate the *Ance* and *Acer* mRNA expression levels simultaneously in adult fruit flies for comparison purposes.

We assessed *Ance* and *Acer*'s mRNA expression levels in eight groups (CD, HFD, HSD, and aging, categorized into females and males) by RT-PCR. Our results show an increase in *Ance* mRNA expression levels in all groups compared to respective control groups (Fig. 5A and B), with a significant increase of eight times in the male aging group (Fig. 5B). Conversely, flies fed with HFD presented a decrease in the *Acer* mRNA expression levels compared with control groups, while flies fed with HSD did not differ from control flies (Fig. 5C and D). Additionally, 40 days-old females demonstrated lower *Acer* mRNA expression levels compared with the young females (Fig. 5C), while 40 days-old males presented 2 times increase compared with the young males (Fig. 5D). These results indicated that *Ance* and *Acer* mRNA expression levels could be regulated by metabolism and age in adult flies [6,42]. Furthermore, HFD-feeding flies presented decreased *Acer* mRNA levels (Fig. 5C and D) along with a more significant decrease in *InR* and *dilp5* mRNA expression levels (Fig. 4) compared to the respective control groups, demonstrating that HFD is more detrimental to metabolism when compared to HSD. This difference could be attributed to the food source type (fat versus sugar) or the calorie amount, considering that in this work, the HFD diet contained almost twice the calorie quantity compared to the HSD diet (Table 1). More studies will be needed to find out the causes of these alterations.

Acer is strongly expressed within the fat body, especially in the head

and abdomen [6]. Even so, flies with higher TAG (Fig. 2E, F, G, and H) did not exhibit increased *Acer* mRNA expression levels; in contrast, they presented increased *Ance* mRNA expression levels (Fig. 5A and B), indicating that fat accumulation in flies from HFD group is not related to *Acer* mRNA expression levels. Meanwhile, *Ance* is highly expressed in the vesicular structures including spermatocytes and immature spermatids [6]. One could expect that *Ance*'s mRNA expression levels would be differently modulated in males and females. Although, both male and female flies from all groups tested showed a significant increase in *Ance* mRNA expression levels. However, the increase in *Ance* mRNA expression levels was almost twice in females (3.37 fold change) than males (1.6 fold change) from the HSD group, while in the aging group males (8.3 fold change) had 3.3 times more *Ance* mRNA expression levels than the females (2.48 fold change) suggesting sex-specific effects on *Ance* mRNA expression levels.

Glover et al. [42] suggested the IIS pathway as a candidate *Acer*-modulated pathway. To better understand the relation between the insulin pathway and *Acer*, we performed correlations between *Acer* and *InR* mRNA expression levels and between *Acer* and *dilp5* mRNA expression levels (Fig. S1). We made the same correlations with the *Ance* gene, despite the absence of data in the literature about its involvement in the IIS pathway (Fig. S2). Our results indicate a positive correlation between *Acer* and *InR* mRNA expression levels in males and female flies (Fig. S1A and B). Similarly, there was a positive correlation between *Acer* and *dilp5* mRNA expression levels in female flies (Fig. S1C), but no correlation between *Acer* and *dilp5* mRNA expression levels in male flies (Fig. S1D). These results suggest a possible involvement of IIS in *Acer* mRNA expression levels, at least in females, although it's not clear how the different diets can modulate this pathway. On the other hand, a negative correlation was observed between *Ance* and *InR* mRNA expression levels as well as *Ance* and *dilp5* mRNA expression levels in male flies. However, there was no correlation between the mRNA expression levels of *Ance* and *InR* and *Ance* and *dilp5* in females.

A recent literature review [6] reported five mechanisms with an overlapping function between Ance or Acer and its human orthologue: Ance was related to fertility and aging; while Acer was related to cardiovascular function, neurodegeneration, and metabolism. In this work,

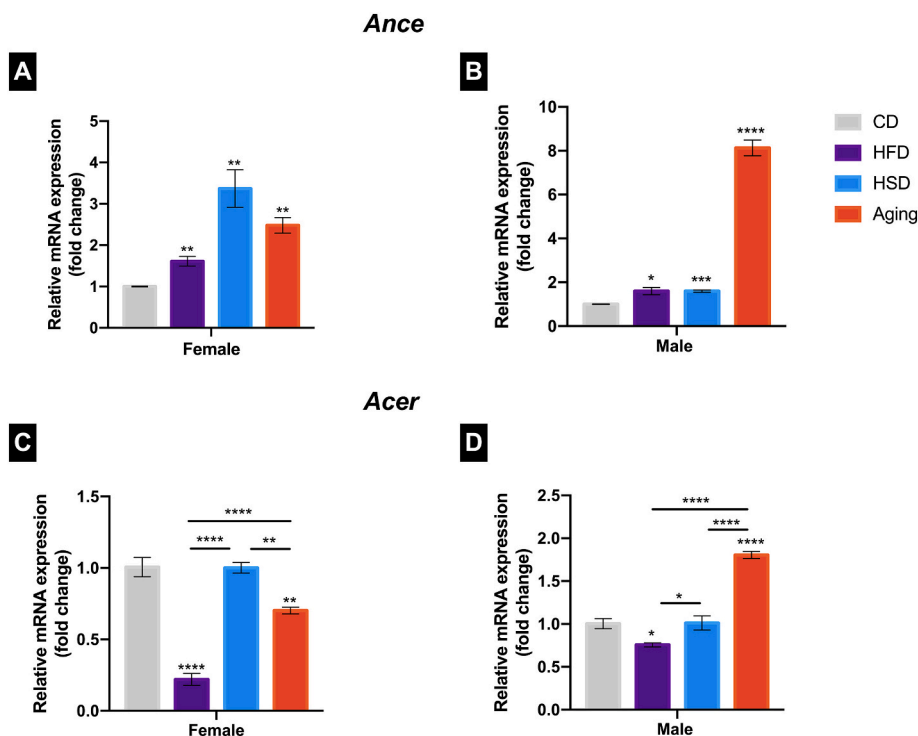


Fig. 5. Relative *Ance* and *Acer* mRNA expression levels on HFD, HSD and aging. The *Ance* gene expression levels in (A) females and (B) males. The *Acer* gene expression levels in (C) female and (D) male ($n = 3-5$ per experimental group). Errors bars indicated means \pm S.E.M. Significance between values for each experimental group and control was determined with a one-way analysis of variance (ANOVA) followed by a Tukey comparisons test, * = $p < 0.05$, ** = $p < 0.01$, *** = $p < 0.001$ and **** = $p < 0.0001$.

all flies' models demonstrated an upregulation of *Ance*'s mRNA expression levels, including elderly flies, with an even more expressive increase in old males (Fig. 5A and B). Although *Acer* has not been related to aging, the male 40 days-old flies showed increased levels of *Acer* mRNA expression levels (Fig. 5C and D). Regarding metabolism, while *Ance* was influenced by both diets, *Acer* was influenced only by HFD, indicating that *Ance* is more responsive to metabolic alterations than *Acer*.

Considering the *Acer* mRNA expression levels in the old flies, *Acer* mRNA expression levels show sexual dimorphism. Old females demonstrated a decrease in their mRNA expression levels of *Acer* compared with young females (Fig. 5C) while there was an increase of almost twice in *Acer* expression levels in males compared with the young males (Fig. 5D). Even though senescence is known to regulate the RAAS positively [4], and there are some studies on the effect of sex on ACE2 levels [48,49], the actual data on ACE2 mRNA expression levels across ages and sex are contradictory [50–52].

The literature on ACE2 in obese or diabetic humans is sparse compared to animal models. For ethical reasons, trial participants do not receive diets high in calories, fat or sugar. Thus, the influence of diet on ACE2 mRNA expression levels is based on interventions by dietary restrictions or weight loss [53,54]. Also, research related to ACE2 mRNA expression levels in organs, such as the heart or liver, is obtained from biopsies [55,56]. These facts reinforce the importance of an animal model for *in vivo* and *ex vivo* COVID-19 studies. Based on the scientific literature and our data, we believe that the alterations in ACE2 orthologs mRNA expression levels observed in the fly models of obesity/DM, and aging, COVID-19 risk groups, may help to elucidate the pathophysiology of this disease. Future studies will be necessary to confirm the role of ACE2 orthologs genes in SARS-CoV-2 infection. Since we analyzed the *Ance* and *Acer* mRNA expression levels for possible ACE2 translational studies, we believe it would be relevant to analyze whether *Ance* and *Acer* proteins could be a potential binding affinity with Spike protein. To predict Spike-*Ance* and Spike-*Acer* interactions, we performed molecular docking.

3.5. *Ance* and *Acer* proteins have predicted interaction affinity with SARS-CoV-2 Spike protein

In 1995, a protein highly homologous to the human ACE was isolated and purified from *D. melanogaster* embryos and called *Ance* [57]. A year later, researchers identified *Acer*, another *D. melanogaster* gene whose predicted translation product shared homology with mammalian

testicular ACE and *Ance* [45]. The sequence identity between ACE and ACE2 is about 40 %, with a similarity of 61 %, as well as in fruit fly orthologs [6,16]. Specifically, comparing ACE and ACE2 values with *Ance* and *Acer*, the amino acid similarity ratio with ACE is 61 % (45 % identity, 48 % coverage) and 58 % (41 % identity, 45 % coverage) with *Ance* and *Acer*, respectively. For ACE2, the similarity with *Ance* is 56 % (36 % identity, 71 % coverage) and with *Acer* is 54 % (35 % identity, 68 % coverage) [6].

Similar to other viruses, the coronavirus needs to become intracellular to use the enzymatic machinery of the host cell and make new virus copies. In this sense, SARS-CoV-2 employs its Spike protein to interact with ACE2 and other cellular proteins [58]. According to Shen et al. [13], a greater affinity between the mutant Spike protein of coronavirus variant B.1.1.7 with the human ACE2 receptor is responsible for the elevated infectivity of the mutant coronavirus. In this work, we evaluated the ACE2 ortholog mRNA expression levels in different fruit fly models and the predicted interaction of their proteins with the SARS-CoV-2 Spike protein. We used the obtained 3D *Acer* and *Ance* protein models to predict the interaction energies complexes at the protein-protein interface between them and SARS-CoV-2 Spike protein. Our molecular docking results show that both proteins have potential sites for interaction with the Spike protein (Fig. 6A and B). The docking binding occurs at different sites: *Acer* exhibited higher binding affinity to the Spike Chain A and C (binding energy of $-921 \text{ kcal mol}^{-1}$), while *Ance* shows higher affinity to the Spike Chain C (binding energy of $-994 \text{ kcal mol}^{-1}$) and appears to make small contacts to the Spike chain B (Fig. 6A and B). Of note, the binding site of *Acer* protein with Spike protein seems to be similar to that found in humans [59,60].

Previous studies demonstrated *in silico* comparisons of the binding affinities of SARS-CoV-2 Spike protein with ACE2 from several species. Interestingly, it was predicted that SARS-CoV-2 could bind ACE2s in various vertebrates, but not in the murine model, demonstrating an advantage in using the fruit fly for COVID-19 studies [61–63]. In addition, a work conducted by Sartore et al. [64] evaluated the interaction between human ACE2 receptors and SARS-CoV-2 Spike protein under different conditions of the hyperglycemic environment through a computational approach. The analysis supports the hypothesis that glycation, a consequence of hyperglycemia in patients affected by DM, could have a role in the SARS-CoV-2 infection, possibly modulating other binding sites for SARS-CoV-2 access into the body. No experimental validation regarding the interaction between *D. melanogaster* ACE-like proteins and Spike protein was performed in the present work. Even so, we believe that further investigations about COVID-19 may

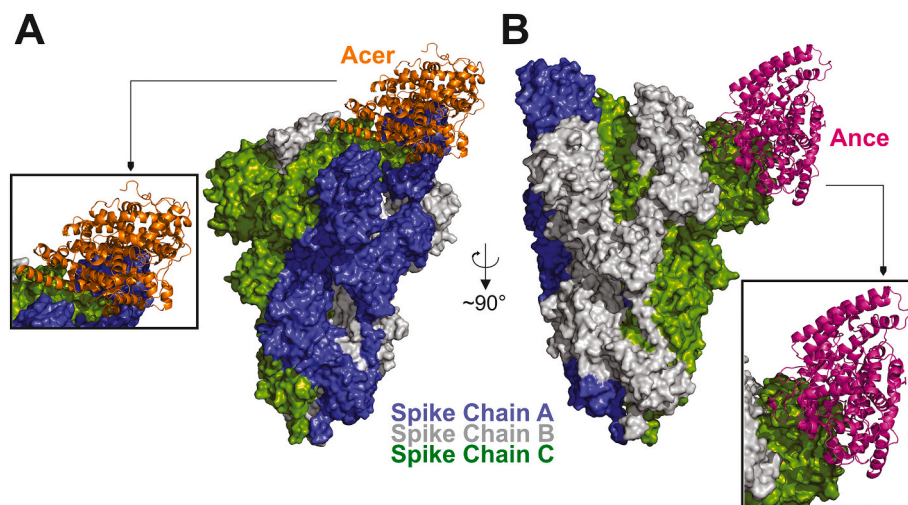


Fig. 6. Docking of *Ance* and *Acer* to the Spike protein. (A) *Acer* docked in the chains A and C of the Spike protein (PDB: 6VSB) [Wrapp, et al., 2020] with a lowest binding energy of $-921 \text{ kcal mol}^{-1}$. The *Acer* 3D structure was predicted using Alpha Fold [Jumper et al., 2021]. (B) *Ance* (PDB: 1J36) [Kim et al., 2003] docked to the chain C of the Spike protein with the lowest binding energy of $-994 \text{ kcal mol}^{-1}$. *Ance* also appears to make small contacts to chain B.

benefit from the analysis provided here.

4. Conclusion

Although it has been more than two years since the COVID-19 epidemic outbreak, there is still a paucity of data on comorbidities and mechanisms that modulate viral pathogenesis. Our work explores the effects of HFD, HSD, and aging on *Ance* and *Acer* mRNA expression levels in the fruit fly. Furthermore, we evaluated by molecular docking whether the interaction of *Ance* and *Acer* proteins with the SARS-CoV-2 Spike protein arises as it occurs with ACE2 in humans. Our study shows that high fat and sugar diets can profoundly affect the weight, glucose, and triglycerides levels, as well as induce insulin resistance in adult flies, which validates our obesity and DM models. Flies at 40 days old had drastically decreased locomotor performance and were used as the aging model. For the first time, *Ance* and *Acer*'s mRNA expression levels were evaluated and compared in different diets, ages, and sexes. Altogether, we show that HFD, HSD, and aging distinctly affected *Ance* and *Acer* gene expression levels in adult flies. Differences between females and males were observed depending on the analysis. Interestingly, both *Ance* and *Acer* proteins have predicted binding regions with the SARS-CoV-2 Spike protein. In summary, these results emphasize the fruit fly as a crucial tool to investigate the pathogenesis of COVID-19, including genetic variations, and to identify new treatments and prevention strategies.

CRedit authorship contribution statement

Conceptualization: T.D., C.L.D.C.; Methodology: T.D., C.L.D.C., M.M.S.; Formal analysis: T.D., C.L.D.C.; Perform experiments: T.D., M.M.S., P.M.; Bioinformatics: B. C. F.; M. D.; Data curation: T.D., C.L.D.C.; Writing - original draft: T.D., C.L.D.C.; Writing - review & editing: T.D., C.L.D.C., N.B.V.B, B. C. F.; M. D.; J.B.T.R; Supervision: C.L.D.C.

Funding

This study was supported by grants from the Coordenação de Aperfeiçoamento de Pesquisa Pessoal de Nível Superior (CAPES EPIDEMIAS 09 #88887.505377/2020) and Fundação de Amparo à Pesquisa do Estado do Rio Grande do Sul (FAPERGS). T.D. (#88887.512883/2020-00) and P.M. (#88887.512821/2020-00) are the recipients of a fellowship from CAPES, and M.D. (19/2551-0001906-8) is the recipient from FAPERGS.

Declaration of competing interest

The authors declare that they have no known competing financial interests or personal relationships that could have appeared to influence the work reported in this paper.

Data availability

Data will be made available on request.

Acknowledgments

We are grateful to Dr. Elgion Lucio da Silva Loreto for providing his laboratory and equipment for RT-PCR analysis and Dr. Barbara Dotto Fontana for the writing suggestions.

Appendix A. Supplementary data

Supplementary data to this article can be found online at <https://doi.org/10.1016/j.bbadis.2022.166551>.

References

- [1] A.J. Pietrobon, F.M.E. Teixeira, M.N. Sato, Immunosenescence and inflammaging: risk factors of severe COVID-19 in older people, *Front. Immunol.* 11 (2020), 579220, <https://doi.org/10.3389/fimmu.2020.579220>.
- [2] S. Gómez-Zorita, I. Milton-Laskibar, L. García-Arellano, M. González, M.P. Portillo, An overview of adipose tissue ACE2 modulation by diet and obesity. Potential implications in COVID-19 infection and severity, *Int. J. Mol. Sci.* 22 (2021) 7975, <https://doi.org/10.3390/ijms22157975>.
- [3] D.J. Drucker, Diabetes, obesity, metabolism, and SARS-CoV-2 infection: the end of the beginning, *Cell Metab.* 33 (2021) 479–498, <https://doi.org/10.1016/j.cmet.2021.01.016>.
- [4] C. Sargiacomo, F. Fotgia, M.P. Lisanti, COVID-19 and chronological aging: senolytics and other anti-aging drugs for the treatment or prevention of corona virus infection? *Aging* 12 (2020) 6511–6517, <https://doi.org/10.18632/aging.103001>.
- [5] S. Beyerstedt, E.B. Casaro, É.B. Rangel, COVID-19: angiotensin-converting enzyme 2 (ACE2) expression and tissue susceptibility to SARS-CoV-2 infection, *Eur. J. Clin. Microbiol. Infect. Dis.* 40 (2021) 905–919, <https://doi.org/10.1007/s10096-020-04138-6>.
- [6] P. Herrera, R.J. Cauchi, ACE and ACE2: insights from drosophila and implications for COVID-19, *Heliyon* 7 (2021), e08555, <https://doi.org/10.1016/j.heliyon.2021.e08555>.
- [7] F. Chaudhry, S. Lavandero, X. Xie, B. Sabharwal, Y.-Y. Zheng, A. Correa, J. Narula, P. Levy, Manipulation of ACE2 expression in COVID-19, *Open Heart* 7 (2020), e001424, <https://doi.org/10.1136/openhrt-2020-001424>.
- [8] F. Triposkiadis, A. Xanthopoulos, G. Giamouzis, K.D. Boudoulas, R.C. Starling, J. Skoularigis, H. Boudoulas, E. Iliodromitis, ACE2, the counter-regulatory renin-angiotensin system axis and COVID-19 severity, *J. Clin. Med.* 10 (2021) 3885, <https://doi.org/10.3390/jcm10173885>.
- [9] L. Lubbe, G.E. Cozier, D. Oosthuizen, K.R. Acharya, E.D. Sturrock, ACE2 and ACE: structure-based insights into mechanism, regulation and receptor recognition by SARS-CoV, *Clin. Sci. (Lond.)* 134 (2020) 2851–2871, <https://doi.org/10.1042/CS20200899>.
- [10] S. Al Heialy, M.Y. Hachim, A. Senok, M. Gaudet, A. Abou Tayoun, R. Hamoudi, A. Alsheikh-Ali, Q. Hamid, Regulation of angiotensin-converting enzyme 2 in obesity: implications for COVID-19, *Front. Physiol.* 11 (2020), 555039, <https://doi.org/10.3389/fphys.2020.555039>.
- [11] C.E. Gómez, B. Perdiguerro, M. Esteban, Emerging SARS-CoV-2 variants and impact in global vaccination programs against SARS-CoV-2/COVID-19, *Vaccines* 9 (2021) 243, <https://doi.org/10.3390/vaccines9030243> (Basel).
- [12] Tracking SARS-CoV-2 variants (n.d.), <https://www.who.int/en/activities/tracking-SARS-CoV-2-variants>. (Accessed 5 May 2022).
- [13] X. Shen, H. Tang, C. McDanal, K. Wagh, W. Fischer, J. Theiler, H. Yoon, D. Li, B. F. Haynes, K.O. Sanders, S. Gnanakaran, N. Hengartner, R. Pajon, G. Smith, F. Dubovsky, G.M. Glenn, B. Korber, D.C. Montefiori, SARS-CoV-2 variant B.1.1.7 is susceptible to neutralizing antibodies elicited by ancestral Spike vaccines, *BioRxiv*, 2021, <https://doi.org/10.1101/2021.01.27.428516>, 2021.01.27.428516.
- [14] J. van de Leemput, Z. Han, *Drosophila*, a powerful model to study virus-host interactions and pathogenicity in the fight against SARS-CoV-2, *Cell Biosci.* 11 (2021) 110, <https://doi.org/10.1186/s13578-021-00621-5>.
- [15] M.T. de Paula, M.R.P. Silva, S.M. Araújo, V.C. Bortolotto, I.K. Martins, G. E. Macedo, J.L. Franco, T. Posser, M. Prigol, *Drosophila melanogaster*: a model to study obesity effects on genes expression and developmental changes on descendants, *J. Cell. Biochem.* 119 (2018) 5551–5562, <https://doi.org/10.1002/jcb.26724>.
- [16] X. Houard, T.A. Williams, A. Michaud, P. Dani, R.E. Isaac, A.D. Shirras, D. Coates, P. Corvol, The *Drosophila melanogaster*-related angiotensin-I-converting enzymes *Acer* and *Ance*—distinct enzymic characteristics and alternative expression during pupal development, *Eur. J. Biochem.* 257 (1998) 599–606, <https://doi.org/10.1046/j.1432-1327.1998.2570599.x>.
- [17] E. Demir, The potential use of *drosophila* as an in vivo model organism for COVID-19-related research: a review, *Turk. J. Biol.* 45 (2021) 559–569, <https://doi.org/10.3906/biy-2104-26>.
- [18] L.P. Musselman, J.L. Fink, K. Narzinski, P.V. Ramachandran, S.S. Hathiramani, R. L. Cagan, T.J. Baranski, A high-sugar diet produces obesity and insulin resistance in wild-type *drosophila*, *Dis. Model. Mech.* 4 (2011) 842–849, <https://doi.org/10.1242/dmm.007948>.
- [19] M.D.W. Piper, L. Partridge, Protocols to study aging in *Drosophila*, *Methods Mol. Biol.* 1478 (2016) 291–302, https://doi.org/10.1007/978-1-4939-6371-3_18.
- [20] A. Ecker, T.K.S. do N. Gonzaga, R.L. Seeger, M.M.D. Santos, J.S. Loreto, A. A. Boligon, D.F. Meinerz, T.H. Lugokenski, J.B.T. da Rocha, N.V. Barbosa, High-sucrose diet induces diabetic-like phenotypes and oxidative stress in *Drosophila melanogaster*: protective role of *Syzygium cumini* and *Bauhinia forficata*, *Biomed. Pharmacother.* 89 (2017) 605–616, <https://doi.org/10.1016/j.biopha.2017.02.076>.
- [21] N.J. Linford, C. Bilgir, J. Ro, S.D. Pletcher, Measurement of lifespan in *Drosophila melanogaster*, *J. Vis. Exp.* (2013) 50068, <https://doi.org/10.3791/50068>.
- [22] J.M. Tennesen, W.E. Barry, J. Cox, C.S. Thummel, Methods for studying metabolism in *Drosophila*, *Methods* 68 (2014) 105–115, <https://doi.org/10.1016/j.jymeth.2014.02.034>.
- [23] A. Hildebrandt, I. Bickmeyer, R.P. Kühnlein, Reliable *Drosophila* body fat quantification by a coupled colorimetric assay, *PLoS One* 6 (2011), e23796, <https://doi.org/10.1371/journal.pone.0023796>.

- [24] M.M. Bradford, A rapid and sensitive method for the quantitation of microgram quantities of protein utilizing the principle of protein-dye binding, *Anal. Biochem.* 72 (1976) 248–254, <https://doi.org/10.1006/abio.1976.9999>.
- [25] M. Jimenez-Del-Rio, C. Guzman-Martinez, C. Velez-Pardo, The effects of polyphenols on survival and locomotor activity in *Drosophila melanogaster* exposed to iron and paraquat, *Neurochem. Res.* 35 (2010) 227–238, <https://doi.org/10.1007/s11064-009-0046-1>.
- [26] P. Desjardins, D. Conklin, NanoDrop microvolume quantitation of nucleic acids, *J. Vis. Exp.* (2010) 2565, <https://doi.org/10.3791/2565>.
- [27] K.J. Livak, T.D. Schmittgen, Analysis of relative gene expression data using real-time quantitative PCR and the 2(-Delta Delta C(T)) method, *Methods* 25 (2001) 402–408, <https://doi.org/10.1006/meth.2001.1262>.
- [28] D. Kozakov, D.R. Hall, B. Xia, K.A. Porter, D. Padhorna, C. Yueh, D. Beglov, S. Vajda, The ClusPro web server for protein-protein docking, *Nat. Protoc.* 12 (2017) 255–278, <https://doi.org/10.1038/nprot.2016.169>.
- [29] I.T. Desta, K.A. Porter, B. Xia, D. Kozakov, S. Vajda, Performance and its limits in rigid body protein-protein docking, *Structure* 28 (2020) 1071–1081.e3, <https://doi.org/10.1016/j.str.2020.06.006>.
- [30] D. Wrapp, N. Wang, K.S. Corbett, J.A. Goldsmith, C.-L. Hsieh, O. Abiona, B. S. Graham, J.S. McLellan, Cryo-EM structure of the 2019-nCoV spike in the prefusion conformation, *Science* 367 (2020) 1260–1263, <https://doi.org/10.1126/science.abb2507>.
- [31] H.M. Kim, D.R. Shin, O.J. Yoo, H. Lee, J.-O. Lee, Crystal structure of *Drosophila* angiotensin I-converting enzyme bound to captopril and lisinopril, *FEBS Lett.* 538 (2003) 65–70, [https://doi.org/10.1016/s0014-5793\(03\)00128-5](https://doi.org/10.1016/s0014-5793(03)00128-5).
- [32] J. Jumper, R. Evans, A. Pritzel, T. Green, M. Figurnov, O. Ronneberger, K. Tunyasuvunakool, R. Bates, A. Židek, A. Potapenko, A. Bridgland, C. Meyer, S.A. Kohli, A.J. Ballard, A. Cowie, B. Romera-Paredes, S. Nikolov, R. Jain, J. Adler, T. Back, S. Petersen, D. Reiman, E. Clancy, M. Zielinski, M. Steinegger, M. Pacholska, T. Berghammer, S. Bodenstein, D. Silver, O. Vinyals, A.W. Senior, K. Kavukcuoglu, P. Kohli, D. Hassabis, Highly accurate protein structure prediction with AlphaFold, *Nature* 596 (2021) 583–589, <https://doi.org/10.1038/s41586-021-03819-2>.
- [33] T. de A. Pinheiro, A.S. Barcala-Jorge, J.M.O. Andrade, T. de A. Pinheiro, E.C. N. Ferreira, T.S. Crespo, G.C. Batista-Jorge, C.A. Vieira, D. de F. Lelis, A.F. Paraíso, U.B. Pinheiro, M. Bertagnoli, C.J.B. Albuquerque, A.L.S. Guimarães, A.M.B. de Paula, A.P. Caldeira, S.H.S. Santos, Obesity and malnutrition similarly alter the renin-angiotensin system and inflammation in mice and human adipose, *J.Nutr. Biochem.* 48 (2017) 74–82, <https://doi.org/10.1016/j.jnutbio.2017.06.008>.
- [34] E.T. Heinrichsen, H. Zhang, J.E. Robinson, J. Ngo, S. Diop, R. Bodmer, W.J. Joiner, C.M. Metallo, G.G. Haddad, Metabolic and transcriptional response to a high-fat diet in *Drosophila melanogaster*, *Mol. Metab.* 3 (2014) 42–54, <https://doi.org/10.1016/j.molmet.2013.10.003>.
- [35] I. Kojta, M. Chacińska, A. Blachnio-Zabielska, Obesity, bioactive lipids, and adipose tissue inflammation in insulin resistance, *Nutrients* 12 (2020) E1305, <https://doi.org/10.3390/nu12051305>.
- [36] S.B. Diop, R.T. Birse, R. Bodmer, High fat diet feeding and high throughput triacylglyceride assay in *Drosophila melanogaster*, *J. Vis. Exp.* (2017), <https://doi.org/10.3791/56029>.
- [37] B.M. Rovenko, N.V. Perkhulyan, D.V. Gospodaryov, A. Sanz, O.V. Lushchak, V. I. Lushchak, High consumption of fructose rather than glucose promotes a diet-induced obese phenotype in *Drosophila melanogaster*, *Comp. Biochem. Physiol. A Mol. Integr. Physiol.* 180 (2015) 75–85, <https://doi.org/10.1016/j.cbpa.2014.11.008>.
- [38] L. Tappy, Metabolism of sugars: a window to the regulation of glucose and lipid homeostasis by splanchnic organs, *Clin. Nutr.* 40 (2021) 1691–1698, <https://doi.org/10.1016/j.clnu.2020.12.022>.
- [39] Aging mechanisms—a perspective mostly from *Drosophila* - Tsurumi - 2020 - *Advanced Genetics* - Wiley Online Library (n.d.), <https://onlinelibrary.wiley.com/doi/full/10.1002/ggn2.10026>. (Accessed 5 May 2022).
- [40] S. Bar, M. Prasad, R. Datta, Neuromuscular degeneration and locomotor deficit in a *Drosophila* model of mucopolysaccharidosis VII is attenuated by treatment with resveratrol, *Dis. Model. Mech.* 11 (2018), dmm036954, <https://doi.org/10.1242/dmm.036954>.
- [41] V. Privalova, E. Szlachcic, E. Sobczyk, N. Szabla, M. Czarnoleski, Oxygen dependence of flight performance in ageing *Drosophila melanogaster*, *Biology* 10 (2021) 327, <https://doi.org/10.3390/biology10040327>.
- [42] Z. Glover, M.D. Hodges, N. Dravec, J. Cameron, H. Askwith, A. Shirras, S. J. Broughton, Loss of angiotensin-converting enzyme-related (ACER) peptidase disrupts behavioural and metabolic responses to diet in *Drosophila melanogaster*, *J. Exp. Biol.* 222 (2019), jeb194332, <https://doi.org/10.1242/jeb.194332>.
- [43] P. Graham, L. Pick, *Drosophila* as a model for diabetes and diseases of insulin resistance, *Curr. Top. Dev. Biol.* 121 (2017) 397–419, <https://doi.org/10.1016/bs.ctdb.2016.07.011>.
- [44] An overview of the insulin signaling pathway in model organisms *Drosophila melanogaster* and *Caenorhabditis elegans* - ScienceDirect (n.d.), <https://www.sciencedirect.com/science/article/pii/S0196978121001480>. (Accessed 5 May 2022).
- [45] C.A.M. Taylor, D. Coates, A.D. Shirras, The Acer gene of *Drosophila* codes for an angiotensin-converting enzyme homologue, *Gene* 181 (1996) 191–197, [https://doi.org/10.1016/S0378-1119\(96\)00503-3](https://doi.org/10.1016/S0378-1119(96)00503-3).
- [46] M. Akif, I. Ntai, E.D. Sturrock, R.E. Isaac, B.O. Bachmann, K.R. Acharya, Crystal structure of a phosphonotriptide K-26 in complex with angiotensin converting enzyme homologue (AnCE) from *Drosophila melanogaster*, *Biochem. Biophys. Res. Commun.* 398 (2010) 532–536, <https://doi.org/10.1016/j.bbrc.2010.06.113>.
- [47] G. Masuyer, M. Akif, B. Czarna, F. Beau, S.L.U. Schwager, E.D. Sturrock, R.E. Isaac, V. Dive, K.R. Acharya, Crystal structures of highly specific phosphinic tripeptide enantiomers in complex with the angiotensin-I converting enzyme, *FEBS J.* 281 (2014) 943–956, <https://doi.org/10.1111/febs.12660>.
- [48] A. Viveiros, M. Gheblawi, P.K. Aujla, D.K. Sosnowski, J.M. Seubert, Z. Kassiri, G. Y. Oudit, Sex- and age-specific regulation of ACE2: insights into severe COVID-19 susceptibility, *J. Mol. Cell. Cardiol.* 164 (2022) 13–16, <https://doi.org/10.1016/j.yjmcc.2021.11.003>.
- [49] E.L.M. Dalpiaz, A.Z. Lamas, I.F. Caliman, R.F.R. Jr, G.R. Abreu, M.R. Moyses, T. U. Andrade, S.A. Gouvea, M.F. Alves, A.K. Carmona, N.S. Bissoli, Correction: sex hormones promote opposite effects on ACE and ACE2 activity, hypertrophy and cardiac contractility in spontaneously hypertensive rats, *PLoS ONE* 10 (2015), e0133225, <https://doi.org/10.1371/journal.pone.0133225>.
- [50] F. Angeli, G. Reboldi, P. Verdecchia, Ageing, ACE2 deficiency and bad outcome in COVID-19, *Clin.Chem.Lab.Med.* 59 (2021) 1607–1609, <https://doi.org/10.1515/cclm-2021-0658>.
- [51] S.A. Baker, S. Kwok, G.J. Berry, T.J. Montine, Angiotensin-converting enzyme 2 (ACE2) expression increases with age in patients requiring mechanical ventilation, *PLoS One* 16 (2021), e0247060, <https://doi.org/10.1371/journal.pone.0247060>.
- [52] R. Rodrigues, S. Costa de Oliveira, The impact of angiotensin-converting enzyme 2 (ACE2) expression levels in patients with comorbidities on COVID-19 severity: a comprehensive review, *Microorganisms* 9 (2021) 1692, <https://doi.org/10.3390/microorganisms9081692>.
- [53] A.G. Izquierdo, M.C. Carreira, H. Boughanem, J.M. Moreno-Navarrete, C. F. Nicoletti, P. Oliver, D. de Luis, C.B. Nonino, M.P. Portillo, M.A. Martinez-Olmos, J.M. Fernandez-Real, F.J. Tinahones, J.A. Martinez, M. Macias-González, F. F. Casanueva, A.B. Crujeiras, Adipose tissue and blood leukocytes ACE2 DNA methylation in obesity and after weight loss, *Eur. J. Clin. Invest.* 52 (2022), e13685, <https://doi.org/10.1111/eci.13685>.
- [54] L. Li, L. Spranger, D. Soll, F. Beer, M. Brachs, J. Spranger, K. Mai, Metabolic impact of weight loss induced reduction of adipose ACE-2 - potential implication in COVID-19 infections? *Metabolism* 154401–154401 (2020).
- [55] J. Soldo, M. Heni, A. Königsrainer, H.-U. Häring, A.L. Birkenfeld, A. Peter, Increased hepatic ACE2 expression in NAFL and Intermittent Outcome Measures In COPD Study (SPIROMICS), NHLBI Trans-Omics for Precision Medicine (TOPMed) Consortium, C. Langelier, P.G. Woodruff, T. Lappalainen, S. A. Christenson, Genetic and non-genetic factors affecting the expression of COVID-19-relevant genes in the large airway epithelium, *Genome Med.* 13 (2021) 66, <https://doi.org/10.1186/s13073-021-00866-2>.
- [56] M.J. Cornell, T.A. Williams, N.S. Lamango, D. Coates, P. Corvol, F. Soubrier, J. Hoheisel, H. Lehrach, R.E. Isaac, Cloning and expression of an evolutionary conserved single-domain angiotensin converting enzyme from *Drosophila melanogaster*, *J. Biol. Chem.* 270 (1995) 13613–13619, <https://doi.org/10.1074/jbc.270.23.13613>.
- [57] J. Yang, S.J.L. Petitjean, M. Koehler, Q. Zhang, A.C. Dumitru, W. Chen, S. Derclaye, S.P. Vincent, P. Soumillion, D. Alsteens, Molecular interaction and inhibition of SARS-CoV-2 binding to the ACE2 receptor, *Nat. Commun.* 11 (2020) 4541, <https://doi.org/10.1038/s41467-020-18319-6>.
- [58] D.J. Benton, A.G. Wrobel, P. Xu, C. Roustan, S.R. Martin, P.B. Rosenthal, J. J. Skehel, S.J. Gamblin, Receptor binding and priming of the spike protein of SARS-CoV-2 for membrane fusion, *Nature* 588 (2020) 327–330, <https://doi.org/10.1038/s41586-020-2772-0>.
- [59] A. Sternberg, C. Naujokat, Structural features of coronavirus SARS-CoV-2 spike protein: targets for vaccination, *Life Sci.* 257 (2020), 118056, <https://doi.org/10.1016/j.lfs.2020.118056>.
- [60] S. Piplani, P.K. Singh, D.A. Winkler, N. Petrovsky, In silico comparison of SARS-CoV-2 spike protein-ACE2 binding affinities across species and implications for virus origin, *Sci. Rep.* 11 (2021) 13063, <https://doi.org/10.1038/s41598-021-92388-5>.
- [61] Y. Qiu, Y.-B. Zhao, Q. Wang, J.-Y. Li, Z.-J. Zhou, C.-H. Liao, X.-Y. Ge, Predicting the angiotensin converting enzyme 2 (ACE2) utilizing capability as the receptor of SARS-CoV-2, *Microbes Infect.* 22 (2020) 221–225, <https://doi.org/10.1016/j.micinf.2020.03.003>.
- [62] J. Damas, G.M. Hughes, K.C. Keough, C.A. Painter, N.S. Persky, M. Corbo, M. Hiller, K.-P. Koepfli, A.R. Pfennig, H. Zhao, D.P. Genereux, R. Swofford, K. S. Pollard, O.A. Ryder, M.T. Nweeia, K. Lindblad-Toh, E.C. Teeling, E.K. Karlsson, H.A. Lewin, Broad host range of SARS-CoV-2 predicted by comparative and structural analysis of ACE2 in vertebrates, *Proc. Natl. Acad. Sci. U. S. A.* 117 (2020) 22311–22322, <https://doi.org/10.1073/pnas.2010146117>.
- [63] G. Sartore, D. Bassani, E. Ragazzi, P. Traldi, A. Lapolla, S. Moro, In silico evaluation of the interaction between ACE2 and SARS-CoV-2 spike protein in a hyperglycemic environment, *Sci. Rep.* 11 (2021) 22860, <https://doi.org/10.1038/s41598-021-02297-w>.